PHYSICAL REVIEW E **70**, 055601(R) (2004)

Anomalous reflections at photonic crystal surfaces

Xiaofang Yu[1] and Shanhui Fan[2]
[1]*Department of Applied Physics, Stanford University, Stanford, California 94305, USA*
[2]*Department of Electrical Engineering, Stanford University, Stanford, California 94305, USA*
(Received 1 April 2004; revised manuscript received 23 August 2004; published 15 November 2004)

We explore the reflection phenomena when a light beam propagating in a photonic crystal is incident upon the interfaces between the crystal and a uniform dielectric. We prove that a generalized wave-vector conservation relation still applies even when the interface is not aligned with special crystal directions. Using this conservation relation, we show that neither the phase velocity nor the group velocity directions of the reflected beam satisfies Snell's law. Rather, the system exhibits remarkable and unusual reflection effects. In particular, total internal reflection is absent except at discrete angular values. The direction of the reflected beam can also be pinned along special crystal directions, independent of the orientation of the interface. And finally, at glancing incidences, strong backward reflections may occur. These effects may be important for creating integrated photonic circuits, and for on-chip image transfer.

DOI: 10.1103/PhysRevE.70.055601 PACS number(s): 42.70.−a

Light reflects at dielectric interfaces. This effect is at the heart of many optical devices such as dielectric mirrors, optical waveguides, and optical fibers. In conventional dielectric systems, the reflection is governed by Snell's law, which states that the angle of reflection is equal to the angle of incidence. Snell's law also dictates the existence of total internal reflection, when a light beam is incident from a high-index to a low-index material, and when the angle of incidence exceeds a certain threshold [1]. In this paper, we explore the reflection phenomena when a light beam propagating in a photonic crystal (PhC) is incident upon the interfaces between the crystal and a uniform dielectric. We show that neither the phase velocity nor the group velocity directions of the reflected beam satisfy Snell's law. Rather, the system exhibits remarkable and unusual reflection effects. In particular, the total internal reflection is absent except at discrete angular values. The direction of the reflected beam can also be pinned along special crystal directions, independent of the orientation of the interface. And finally, at glancing incidences, strong backward reflections may occur. Some of these effects are unique properties of PhC and cannot be observed in any uniform anisotropic medium.

An example of a PhC-dielectric interface is shown in the inset of Fig. 1; we consider a wave incident upon the interface with a definite Bloch wave vector $\boldsymbol{k}$ in the crystal. In general, when the interface is not aligned with respect to a special crystal direction, the dielectric structure, including both the crystal and the interface, is not periodic. Nevertheless, the wave vector of the reflected wave can be obtained by solving the equation

$$\boldsymbol{k}_p^{inc}(\omega) = \boldsymbol{k}_p^{ref}(\omega) + \boldsymbol{G}_p, \tag{1}$$

where $\boldsymbol{k}_p^{inc}, \boldsymbol{k}_p^{ref}$ are the wave-vector components parallel to the interface for the incident and the reflected waves in the

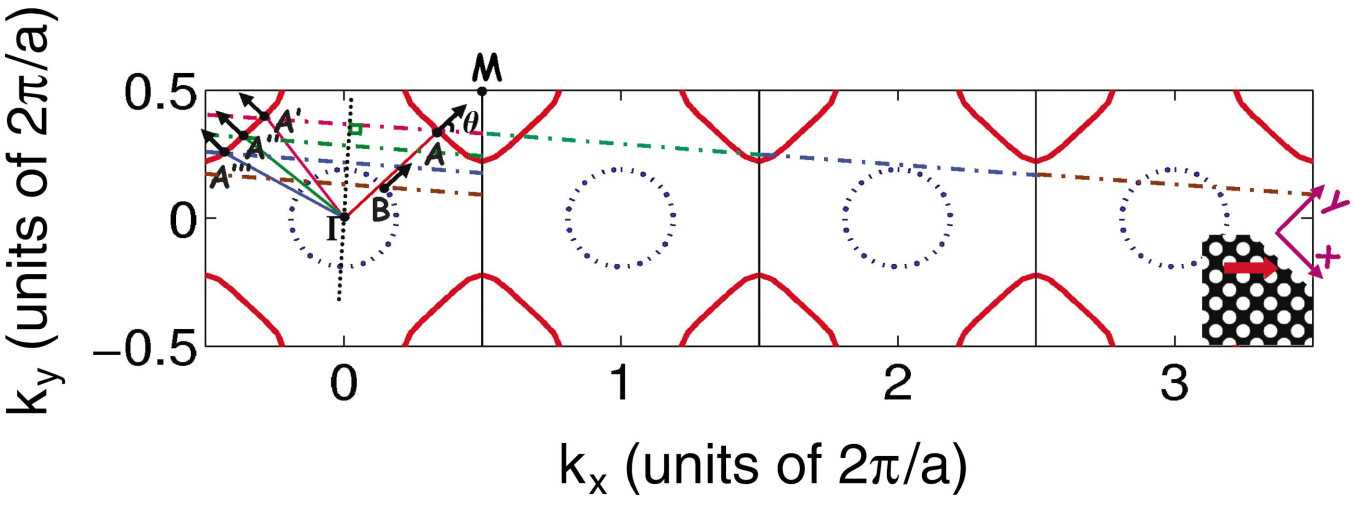

FIG. 1. (Color) Constant frequency contour for the photonic crystal structure shown in the inset, which consists of a square lattice of air holes introduced in the dielectric ($\varepsilon=12$). The red arrow in the inset indicates the incidence of a plane wave. The red solid lines represent the contour at $f=0.19(c/a)$. The dashed circles are the CFC for air at $f=0.19(c/a)$. The dotted line is parallel to the interface, and point A represents the wave vector of the incident wave. The line that passes through point A in a direction perpendicular to the interface is the k-conservation line. The intersections of such line with the constant frequency contour determine the wave vectors of the reflected wave.

crystal and $\boldsymbol{G}_p$ is the parallel component of any reciprocal lattice vector. The proof is as follows: for the truncated crystal as shown in the inset of Fig. 1, the dielectric function is

$$\boldsymbol{\varepsilon}(\boldsymbol{r}_p, r_n) = \begin{cases} \boldsymbol{\varepsilon}_{crystal}(\boldsymbol{r}_p, r_n) \equiv \sum_G \boldsymbol{\varepsilon}_G \exp(i\boldsymbol{G}_p\boldsymbol{r}_p + iG_n r_n) & (r_n < 0) \\ \boldsymbol{\varepsilon}_{air}(\boldsymbol{r}_p, r_n) = 1 & (r_n > 0) \end{cases} \tag{2}$$

where $\boldsymbol{G}$ is a reciprocal lattice vector of the PhC. Fourier transforming $\boldsymbol{\varepsilon}^{-1}(\boldsymbol{r}_p, r_n)$, we have

$$\begin{aligned} \varepsilon^{-1}(\boldsymbol{f}_p, f_n) &= \int_{-\infty}^{0} dr_n \int_{-\infty}^{+\infty} \sum_G \varepsilon_G^{-1} \\ &\quad \times \exp(i\boldsymbol{G}_p\boldsymbol{r}_p + iG_n r_n)\exp(-i\boldsymbol{f}_p\boldsymbol{r}_p - if_n r_n)d\boldsymbol{r}_p \\ &\quad + \int_{0}^{+\infty} dr_n \int_{-\infty}^{+\infty} \exp(-i\boldsymbol{f}_p\boldsymbol{r}_p - if_n r_n)d\boldsymbol{r}_p \\ &= \sum_G A(f_n, G_n)\delta(\boldsymbol{f}_p - \boldsymbol{G}_p) + B(f_n)\delta(\boldsymbol{f}_p) \\ &= \sum_G C(f_n, G_n)\delta(\boldsymbol{f}_p - \boldsymbol{G}_p), \end{aligned} \tag{3}$$

where A, B, C are functions of f_n, G_n. Thus, the Fourier coefficient is nonzero only for a discrete set of wave vectors $\{\boldsymbol{G}_p\}$. (The set $\{\boldsymbol{G}_p\}$, being the projection of the reciprocal lattice vectors along the directions parallel to the surface, is nonperiodic in general.) By expressing the master equations for the magnetic field in the wave-vector domain and by equating the coefficients for each Fourier component on both sides of the equation [2], one can show that the solution for the magnetic field has the form

$$\boldsymbol{H}_{\boldsymbol{k}_p}(\boldsymbol{r}_p, r_n) = \sum_G S(\boldsymbol{k}_p - \boldsymbol{G}_p, r_n)\exp[\mathrm{i}(\boldsymbol{k}_p - \boldsymbol{G}_p)\cdot\boldsymbol{r}_p]. \tag{4}$$

At the crystal-air interface, a wave with parallel wave vector $\boldsymbol{k}_p$ therefore only couples to waves with parallel wave vectors $\boldsymbol{k}_p - \boldsymbol{G}_p$.

We graphically solve Eq. (1), by plotting $\omega(\boldsymbol{k})$ in a constant frequency contour (CFC) representation. Previously, it has been shown that the complex band structures $\omega(\boldsymbol{k})$ in PhC lead to a variety of propagation effects such as self-collimation, superprism, and negative refraction [3–17]. Here, using the band structure $\omega(\boldsymbol{k})$ in combination with Eq. (1), we explore the effects of spatial dispersion in photonic crystal on the reflection properties. As an example, we consider a crystal as shown in the inset of Fig. 1, which consists of a square lattice of air holes introduced into a high-index semiconductor material with $\varepsilon = 12$. The holes have a radius of $0.35a$, where a is the lattice constant. For such a crystal, the CFC for the transverse electric waves in the first band is shown in Fig. 1 for a frequency $f = 0.19(c/a)$. At this frequency, the shape of the crystal CFC can be approximated as squares around the M point [9,12]. Thus, self-collimation occurs along the [11] direction [11,13,16,17], which facilitates our computational study to be presented later.

To illustrate the procedure of determining the reflected wave, we consider a wave propagating along the [11] direction inside the PhC at frequency $f = 0.19(c/a)$, as represented by point A in Fig. 1. The wave is incident upon a crystal truncation, whose direction is represented by a dashed line. Outside the truncation the medium is assumed to be air (Fig. 1). The choice of the medium outside affects the reflection coefficient, but not the wave vector of the reflected beams. By drawing a "k-conservation" line through A in a direction perpendicular to the interface, we search for the intersections of such k-conservation line with the CFC to determine the reflected wave vector. Since the band structure is periodic in the $\boldsymbol{k}$ space, i.e., $\omega(\boldsymbol{k}) = \omega(\boldsymbol{k} + \boldsymbol{G})$, multiple reflected waves A', A'', A''',… may occur. This is represented in the reduced-zone scheme by translating into the first Brillouin zone the portions of the k-conservation line that lie outside. Also, when the k-conservation line intersects the air CFC (for example, point B in Fig. 1), radiation loss into the air occurs. In general, due to the complex shapes of the frequency contour in the PhC, neither the phase-velocity nor the group-velocity directions of the reflected wave satisfy Snell's law. In the following discussions, we present a set of remarkable reflection phenomena as we vary the orientation of the PhC-air interface.

We start from the case $\theta = 45°$, where θ is the incident angle. In this case, a PhC-air interface is introduced by truncating the PhC at a (10) plane. The k-conservation line intersects the CFC for PhC only at a single location [point A' in Fig. 2(a)] in the reduced-zone scheme. This point corresponds to the reflected wave with a wave vector and a group velocity along the $[\bar{1}1]$ direction. Thus the incident wave is bent by 90°, and the incident angle is equal to the angle of reflection. Since the k-conservation line stays outside of the CFC for air, total internal reflection occurs and the bending efficiency is 100%, as confirmed by our previous numerical study [16]. Furthermore, such a bend substantially preserves modal shape. A finite beam propagating along the [11] direction consists of multiple wave vectors around point A [for example, point B in Fig. 2(a)]. During the bending process, there is a one-to-one mapping between the incident and reflected wave vectors. Also, such mapping preserves the distances between the multiple $\boldsymbol{k}$ points (i.e., $|\boldsymbol{k}_A - \boldsymbol{k}_B| = |\boldsymbol{k}_{A'} - \boldsymbol{k}_{B'}|$). Consequently the modal shape is substantially preserved. All these effects can be seen in Fig. 2(b), where an incident beam with an odd modal profile is bent into an odd mode in the outgoing direction, in spite of the lack of mirror symmetry of the overall structure along the beam propagation directions. Thus, self-collimation beam provides the capability to route optical images on-chip through sharp 90° bends, which would be difficult to accomplish in either multimode waveguides or arrays of single-mode waveguides.

When the orientation of the interface deviates slightly from the (10) plane, a wave that is propagating along the [11] direction will no longer be reflected into a wave with a wave vector along the $[\bar{1}1]$ direction. However, as we can see from Fig. 1, which corresponds to the case when the incident angle $\theta = 48°$, the reflected wave vector still lies at the flat region of the constant frequency contour. Consequently the group velocity direction of the reflected wave is pinned along

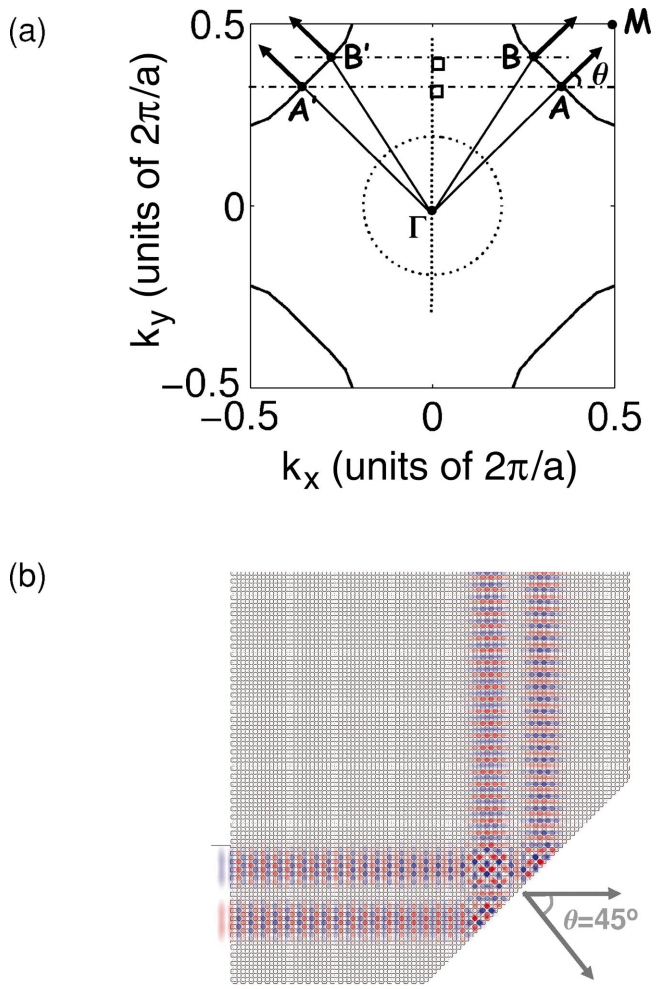

FIG. 2. (Color) (a) The CFC plot for the case when the incident wave has a wave vector around point *A* along the [11] direction. The interface is chosen along the (10) plane such that the incident angle $\theta=45°$. (b) Steady-state magnetic field pattern for the case $\theta=45°$. A dielectric waveguide represented by the rectangle excites a beam inside the photonic crystal. Red and blue represent large positive and negative amplitudes, respectively.

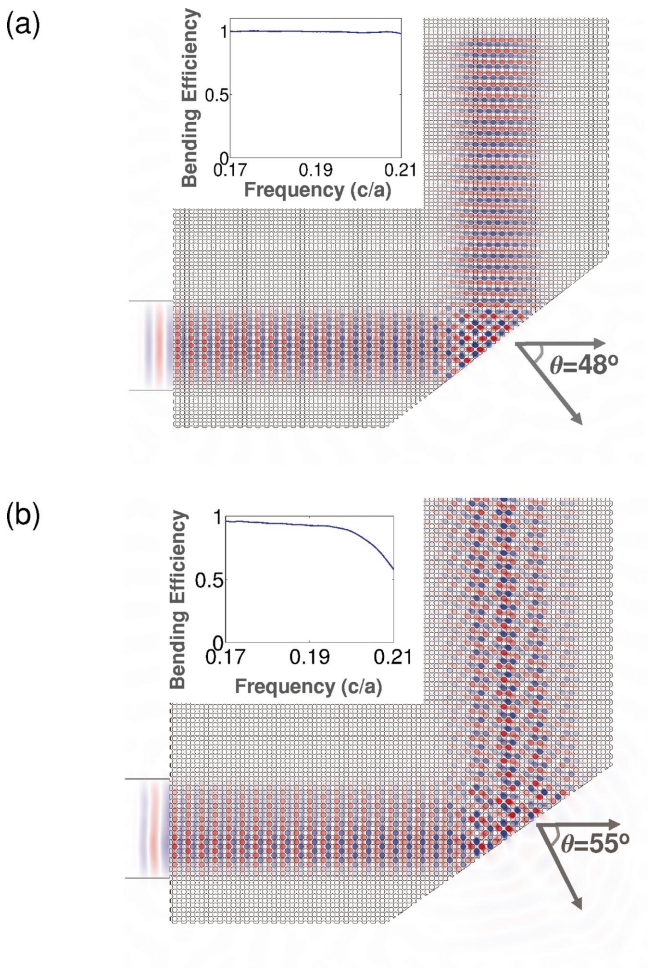

FIG. 3. (Color) Steady-state magnetic field pattern for (a) $\theta=48°$, (b) $\theta=55°$. The inset shows the corresponding bending efficiency.

the $[\bar{1}1]$ direction of the crystal, and is independent of the orientation of the interface. This effect can be seen in the steady state field pattern generated by FDTD simulation shown in Fig. 3(a). Slightly reducing the incident angle also produces similar pinning behavior. In these cases, multiple reflected wave vectors can be generated for a single incident wave vector, and for each reflected wave vector the angle between the phase velocity and the group velocity is different from the angle for the corresponding incident wave vector. Thus the beam shapes are no longer preserved after the bending and instead depend upon the orientation of the interface.

To determine the reflectivity of the interfaces, we apply a pulse propagation technique in FDTD simulations [16]. We send in a pulse with a cross-section dimension of approximately 14*a*, and with a spatial profile of a fundamental mode of a dielectric-slab waveguide. We employ a large crystal in the calculation, such that the parasitic reflected pulse from other crystal boundaries can be temporally filtered out, and the results represent the intrinsic characteristics of the interface only [11]. The bending efficiency of the interface is determined by normalizing the bent power with respect to the incident power. As shown in the inset of Fig. 3(a), the efficiency is very close to 100% in the entire frequency range where self-collimation occurs.

Recently, the use of self-collimation beams has been shown to be an important and effective mechanism for creating on-chip integrated photonic circuits [14–16]. In this context, the pinning effects discovered here indicate that the reflection is quite robust against small errors in crystal surface orientations. Thus, unlike typical free-space optics, here one need not align the mirror perfectly in order for the beam to be routed along specific directions, which simplifies the practical implementations of on-chip circuits.

While in the FDTD simulations near 100% bending efficiency is observed when the interface slightly deviates from (10) surface, we note that except for the special case when the interface lies exactly on the (10) plane, the bending cannot be perfect. In the general cases, the *k*-conservation line always intersects the CFC for air (Fig. 1), and radiation into the air will inevitably exist. Total internal reflection thus occurs only for interfaces with special orientations. When the

deviation from the (10) plane is small, the intersections of the *k*-conservation line and the air CFC occur in higher-order Brillouin zones. Consequently the radiation loss is small and the reflection coefficients are still very close to 100%, as our simulations indicate. At larger angles of incidence, the breakdown of total internal reflection becomes more evident. Figure 3(b) shows the bending efficiency and the steady state field pattern for the case of $\theta=55°$, where the reflected beam is still pinned along the $[\bar{1}1]$ direction but substantial radiation loss into the air at the PhC-air interface is observed.

At even larger incidence angles, the incident beam can be reflected backwards. This unusual effect can be observed at $\theta=70°$, where the *k*-conservation line intersects the crystal CFC at a region that corresponds to backward propagating waves. The fact that the reflected wave is propagating backwards can be more easily seen with a translation into the first Brillouin zone by a reciprocal lattice vector (Fig. 4). In addition to the backward waves, there exist reflections to other directions (for example, point *B* in Fig. 4, which corresponds to the wave bent by 90°) and radiations into the air (for example, point *C*, which corresponds to the radiation into the air). Nevertheless, the FDTD simulations reveal that about 80% of the incident power is sent backwards. The backward wave has the same beam shape as the incident wave (Fig. 4), when a special incident angle is chosen such that the incident wave vector along the [11] direction is mapped to the center of the flat region that corresponds to the $[\bar{1}1]$ direction. The existence of such backward waves result directly from the presence of multiple manifolds in the $\omega(\mathbf{k})$ diagram in photonic crystals and cannot be observed in typical anisotropic media.

As closing remarks, the procedure for determining the reflected wave outlined here can be straightforwardly applied to either photonic crystal slab structure or three-dimensional (3D) photonic crystals, since the directions of the reflected waves depend only upon the band structure in the crystal. We use the first band of a two-dimensional (2D) crystal. It has been shown that the first band of a corresponding photonic crystal slab has very similar dispersion characteristics, and lies below the light cone of the air [11]. Thus there is no vertical radiation for both propagating beam in the crystal and reflection properties in the case of the [10] interface. We have actually performed 3D FDTD simulations as well, and indeed see negligible vertical radiations in these cases [18].

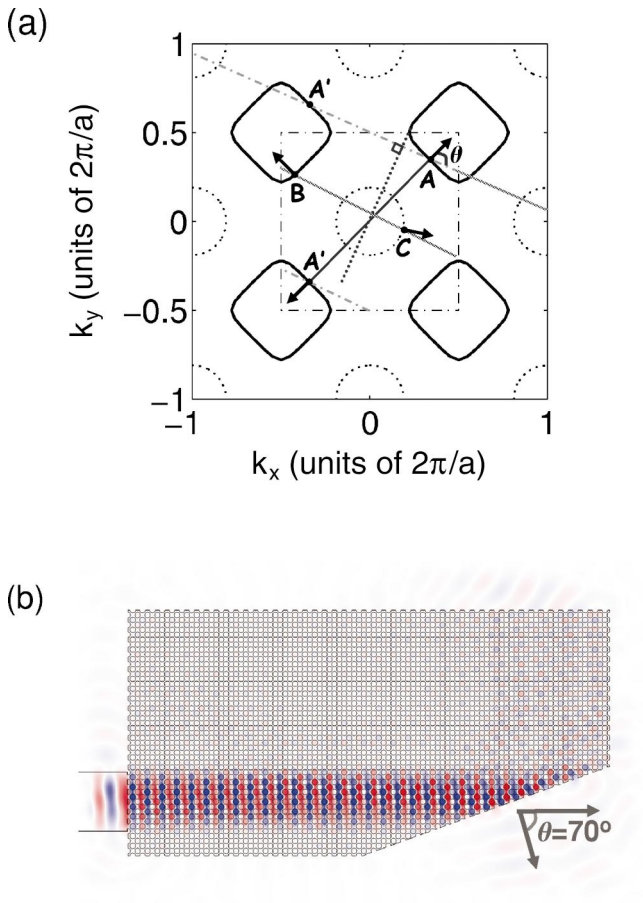

FIG. 4. (Color) (a) CFC plot for the case $\theta=70°$. (b) Steady-state field pattern for the case $\theta=70°$. Notice the presence of strong backward reflection.

This work was funded in part by the National Science Foundation (NSF) Grant No. ECS-0200445, an ARO-MURI grant No. DAAD19-03-1-0227, and the David and Lucile Packard Foundation. The simulations were performed through the support of a NSF-NRAC program. X.Y. acknowledges the support of a Herb and Jane Dwight program.

[1] B. E.A. Saleh *et al.*, *Fundamentals of Photonics* (Wiley, New York, 1991).
[2] J.D. Joannopoulos, R.D. Meade, and J.N. Winn, *Photonic Crystals* (Princeton University Press, 2003).
[3] P. St. J. Russell, Appl. Phys. B: Photophys. Laser Chem. **B39**, 231 (1986).
[4] R. Zengerle, J. Mod. Opt. **34**, 1589 (1987).
[5] S. Enoch *et al.*, Opt. Commun. **161**, 1589 (1987).
[6] S. Y. Lin *et al.*, Opt. Lett. **21**, 1771 (1996).
[7] H. Kosaka *et al.*, Phys. Rev. B **58**, R10096 (1998).
[8] H. Kosaka *et al.*, Appl. Phys. Lett. **74**, 1212 (1999).
[9] M. Notomi, Phys. Rev. B **62**, 10696 (2000).
[10] M. C. Netti *et al.*, Phys. Rev. Lett. **86**, 1526 (2001).
[11] J. Witzens *et al.*, IEEE J. Sel. Top. Quantum Electron. **8**, 1246 (2002).
[12] C. Luo *et al.*, Phys. Rev. B **65**, 201104 (2002).
[13] J. Witzens and A. Scherer, J. Opt. Soc. Am. A **20**, 935 (2003).
[14] L. Wu *et al.*, J. Lightwave Technol. **21**, 561 (2003).
[15] D. Chigrin *et al.*, Opt. Express **11**, 1203 (2003).
[16] X. Yu and S. Fan, Appl. Phys. Lett. **83**, 3251 (2003).
[17] C. Chen *et al.*, Opt. Express **11**, 3153 (2003).
[18] W. Lau, X. Yu, and S. Fan (unpublished).